Phosphorylation of moesin by Jun N-terminal kinase is important for podosome rosette formation in Src-transformed fibroblasts

Yi-Ru Pan[1], Wei-Shan Tseng[2], Po-Wei Chang[1] and Hong-Chen Chen[1,2,3,4,*]

[1]Department of Life Sciences, National Chung Hsing University, Taichung 40227, Taiwan
[2]Graduate Institute of Biomedical Sciences, National Chung Hsing University, Taichung 40227, Taiwan
[3]Agricultural Biotechnology Center, National Chung Hsing University, Taichung 40227, Taiwan
[4]Rong-Hsing Research Center for Translational Medicine, National Chung Hsing University, Taichung 40227, Taiwan
*Author for correspondence (hcchen@nchu.edu.tw)

Accepted 20 September 2013
Journal of Cell Science 126, 5670–5680

doi: 10.1242/jcs.134361

Summary

Podosomes are actin-based membrane protrusions that facilitate extracellular matrix degradation and motility of invasive cells. Podosomes can self-organize into large rosette-like structures in Src-transformed fibroblasts, osteoclasts and some highly invasive cancer cells. However, the mechanism of this assembly remains obscure. In this study, we show that the suppression of Jun N-terminal kinase (JNK) by the JNK inhibitor SP600125 or short-hairpin RNA inhibited podosome rosette formation in SrcY527F-transformed NIH3T3 fibroblasts. In addition, SrcY527F was less able to induce podosome rosettes in JNK1-null or JNK2-null mouse embryo fibroblasts than in wild-type counterparts. The kinase activity of JNK was essential for promoting podosome rosette formation but not for its localization to podosome rosettes. Moesin, a member of the ERM (ezrin, radixin and moesin) protein family, was identified as a substrate of JNK. We show that the phosphorylation of moesin at Thr558 by JNK was important for podosome rosette formation in SrcY527F-transformed NIH3T3 fibroblasts. Taken together, our results unveil a novel role of JNK in podosome rosette formation through the phosphorylation of moesin.

Key words: JNK, ERM, Moesin, Podosome rosettes, Phosphorylation

Introduction

Podosomes are actin-based membrane protrusions at the ventral cell surface that promote invasive motility of several types of normal cells, including macrophages, dendritic cells, vascular smooth muscle cells, osteoclasts and endothelial cells (Murphy and Courtneidge, 2011). Many invasive cancer cells display structures similar to podosomes, called invadopodia, which represent the major sites of extracellular matrix degradation in these cells (Caldieri and Buccione, 2010). Each podosome is composed of an actin core surrounded by integrins and integrin-associated proteins such as paxillin. The assembled podosomes recruit matrix metalloproteinases (MMPs) and facilitate focal degradation of extracellular matrix and invasion (Linder et al., 2011). Podosomes are displayed as dot- or rosette-like structures. Podosome dots can undergo self-organization into podosome rosettes in Src-transformed fibroblasts, osteoclasts, endothelial cells and some highly invasive cancer cells. Podosome rosettes are much more potent than podosome dots in promoting matrix degradation (Pan et al., 2011).

ERM (ezrin, radixin and moesin) proteins are closely related members of the band 4.1 superfamily, which crosslink the actin cytoskeleton to several transmembrane proteins (Arpin et al., 2011). The N-terminal halves of these proteins contain the FERM (4.1 ERM) domain and bind directly to CD44 (Legg and Isacke, 1998; Tsukita et al., 1994), the Na^+/H^+-exchanger NHE1 (Denker et al., 2000), CD43 (Serrador et al., 1998) and intercellular adhesion molecules (ICAMs; Heiska et al., 1998; Serrador et al., 1997; Yonemura et al., 1998). The N-termini of ERM proteins associate and mask the C-termini through an intramolecular interaction (Matsui et al., 1998). Phosphorylation of ERM proteins at the conserved threonine residue in the C-termini (Thr567 in ezrin, Thr564 in radixin and Thr558 in moesin) allows these proteins to be relieved from the intramolecular interaction (Ng, et al., 2001; Oshiro et al., 1998; Simons et al., 1998). The C-termini of ERM proteins interact with actin filaments, thereby linking the actin cytoskeleton to the plasma membrane (Tsukita and Yonemura, 1999). ERM proteins have been implicated in various cellular functions that involve cytoskeletal and membrane remodeling, such as cell adhesion and migration (Arpin et al., 2011). Notably, ezrin was shown to be important for podosome rosette formation in PaCa3 pancreatic cancer cells (Kocher et al., 2009).

Jun NH_2-terminal kinase (JNK) is a member of the mitogen-activated protein kinase family, which responds to environmental stresses, cytokines and growth factors (Manning and Davis, 2003). JNK proteins are encoded by three genes (*Mapk8*, *Mapk9* and *Mapk10*) that give rise to at least ten isoform proteins by alternative RNA splicing (Gupta et al., 1996). JNK1 and JNK2 proteins are ubiquitously expressed, but JNK3 is predominantly detected in the brain (Brecht et al., 2005). JNKs are activated by MKK4 and MKK7, which phosphorylate the dual motif (Thr183/Tyr185) of JNK (Davis, 2000). JNK-interacting protein 1 (JIP1) enhances JNK activation by acting as a scaffold protein for

MAPKK–MKK4/7–JNK signaling modules (Whitmarsh et al., 1998). Active JNK proteins are present in both the nucleus and cytoplasm, where they phosphorylate various substrates to regulate different cell functions, including cell proliferation, apoptosis and cell movement (Bogoyevitch and Kobe, 2006). In the nucleus, JNK regulates gene expression by phosphorylating and activating transcriptional factors such as AP1 proteins (Eferl and Wagner, 2003). In the cytoplasm, JNK participates in the regulation of apoptosis and cell motility. JNK has been shown to modulate apoptosis by phosphorylating 14-3-3 proteins and Bcl2 family proteins (Tsuruta et al., 2004). In addition, JNK has been reported to promote cell motility by directly phosphorylating the focal adhesion protein paxillin (Huang et al., 2003) or microtubule-associated proteins MAP2 and MAP1B (Chang et al., 2003). The phosphorylation of paxillin at Ser178 by JNK increases focal adhesion turnover and cell migration (Huang et al., 2003).

It is generally believed that JNK promotes cell invasion by activating the transcriptional factor AP1 and the expression of MMPs (Manning and Davis, 2003; Cheung et al., 2006; Wu et al., 2009). Paxillin is known to be required for podosome/invadopodia formation (Badowski et al., 2008); therefore, we investigated whether JNK plays a role in podosome formation by phosphorylating paxillin. In this study, we found that both JNK1 and JNK2 are important for the formation of podosome rosettes in Src-transformed fibroblasts. However, in this regard, paxillin does not mediate the effect of JNK. Instead, we identified the ERM protein moesin as a novel substrate for JNK and demonstrated that the phosphorylation of moesin at Thr558 by JNK is important for podosome rosette formation.

Results

Both JNK1 and JNK2 are important for podosome rosette formation in Src-transformed fibroblasts

Src-transformed fibroblasts have been used as a model to study the formation of podosome rosettes. In this study, rosette- and dot-like podosomes were visualized at the ventral surface of SrcY527F-transformed NIH3T3 fibroblasts by total internal reflection microscopy and their 3D images were reconstituted by confocal microscopy (supplementary material Fig. S1). We found that the JNK inhibitor SP600125 but not the MEK1 inhibitor PD98059 suppressed the formation of podosome rosettes in SrcY527F-transformed NIH3T3 fibroblasts (Fig. 1A,B), suggesting that the activity of JNK but not ERK is

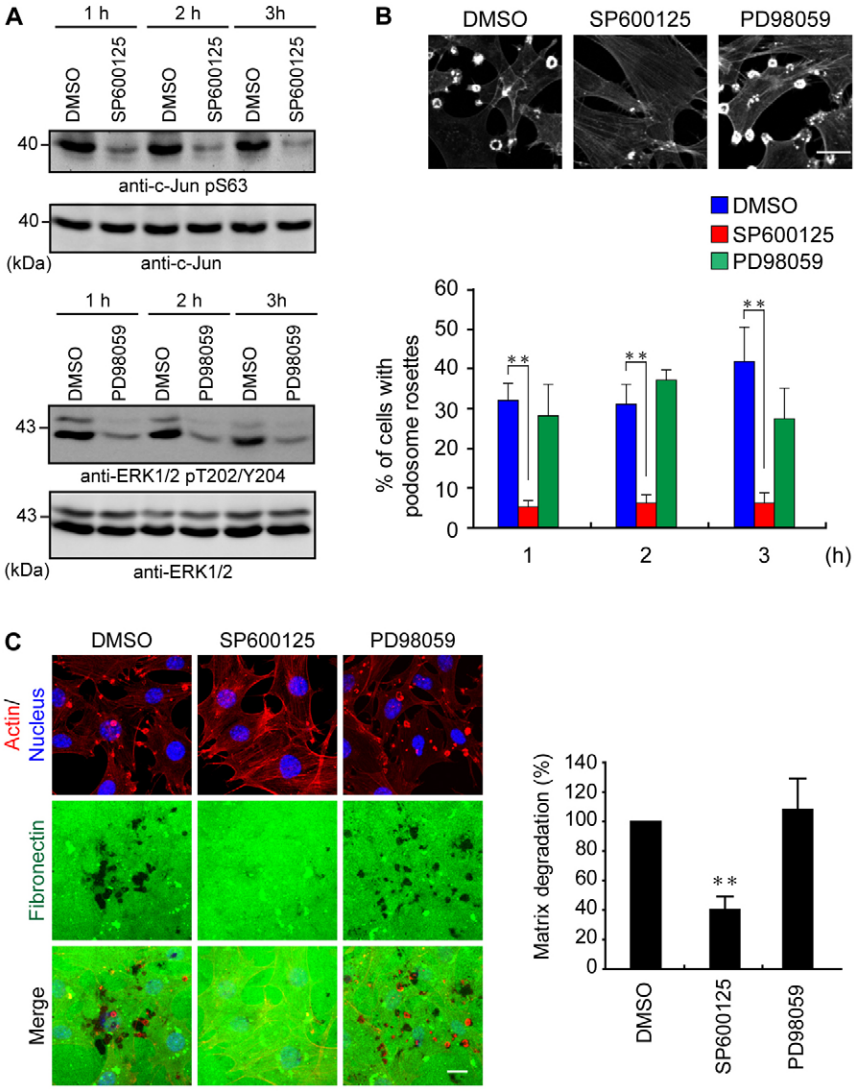

Fig. 1. The JNK inhibitor SP600125 suppresses the formation of podosome rosettes in SrcY527F-transformed NIH3T3 fibroblasts. (A) SrcY527F-transformed NIH3T3 cells were grown for 24 hours and then treated with 25 μM SP600125 (a JNK inhibitor) or 25 μM PD98059 (a MEK1 inhibitor) for 1, 2 or 3 hours. For the control, an equal volume of the solvent DMSO was added to the medium. An equal amount of whole-cell lysates was analyzed by immunoblotting with the indicated antibodies. (B) SrcY527F-transformed NIH3T3 cells were grown on fibronectin-coated glass coverslips for 24 hours and then treated with 25 μM SP600125 or 25 μM PD98059 for 1, 2 or 3 hours. The cells were fixed and stained for F-actin. The percentage of cells containing podosome rosettes in the total number of counted cells was determined ($n \geq 500$). Values (means ± s.d.) are based on three independent experiments; $^{**}P<0.005$. (C) SrcY527F-transformed NIH3T3 cells were grown on glass coverslips coated with Alexa-Fluor-488-conjugated fibronectin and treated with 25 μM SP600125 or 25 μM PD98059 for 12 hours. The cells were fixed and stained for F-actin and nuclei. The dark areas on the images (middle row; fibronectin) represent the areas where the Alexa-Fluor-488-conjugated fibronectin was degraded. The degraded areas from 10 random fields were measured and expressed as the percentage relative to the level in control DMSO-treated cells, which was defined as 100%. Values (means ± s.d.) are based on at least three independent experiments; $^{**}P<0.005$. Scale bars: 20 μm.

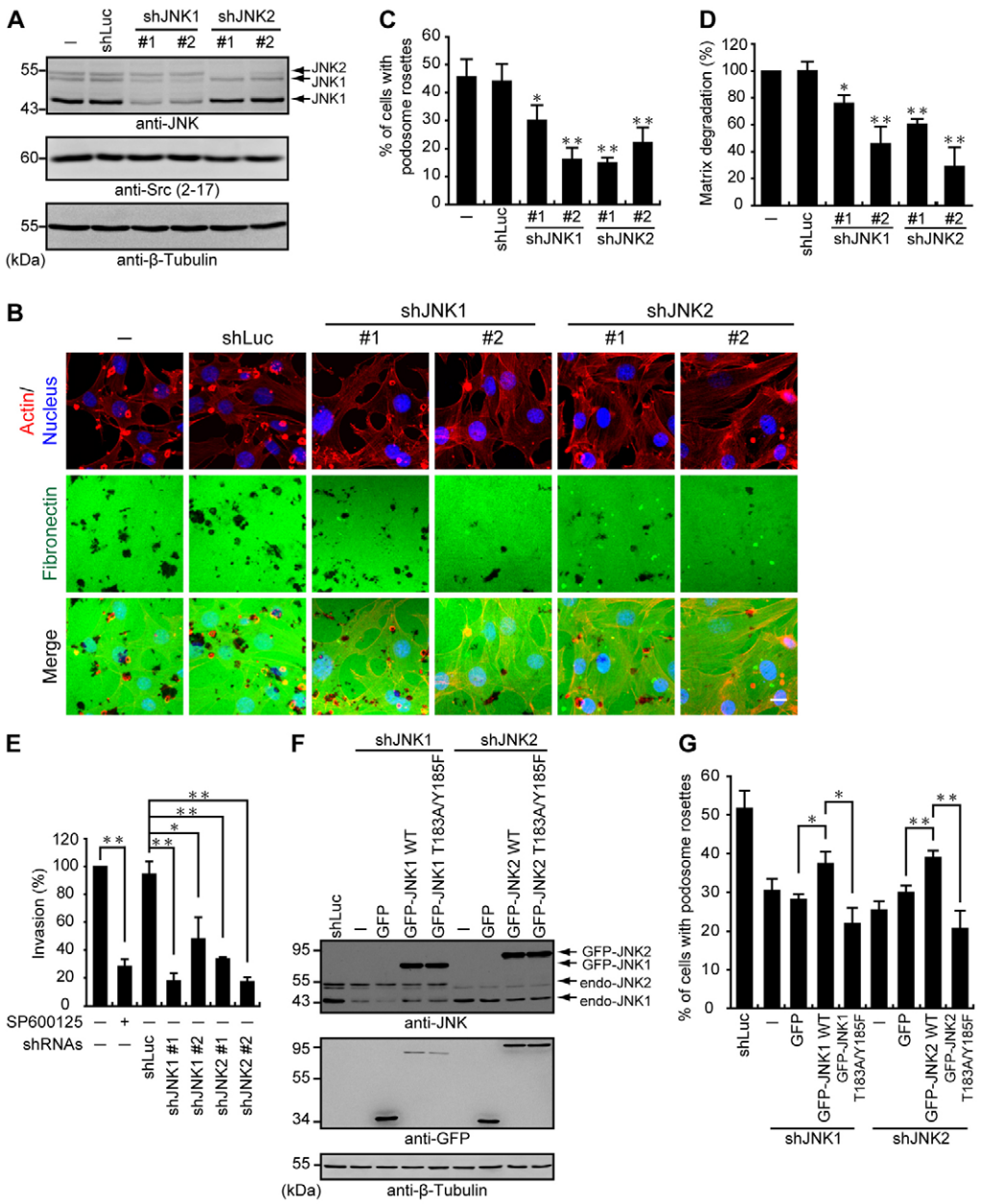

Fig. 2. Depletion of JNK decreases podosome rosette formation in SrcY527F-transformed NIH3T3 fibroblasts. (A) SrcY527F-transformed NIH3T3 cells were infected with recombinant lentiviruses encoding shRNAs specific to luciferase (shLuc), JNK1 (shJNK1; clones #1 and #2) or JNK2 (shJNK2; clones #1 and #2). Equal amounts of whole-cell lysates were analyzed by immunoblotting with the indicated antibodies. (B) The cells as in panel A were grown on Alexa-Fluor-488-conjugated fibronectin for 24 hours. The cells were fixed and stained for F-actin and nuclei. Scale bar: 20 μm. (C) Quantitative results of podosome rosette formation in B. The percentage of cells containing podosome rosettes in the total number of counted cells was determined ($n \geq 200$). Values (means ± s.d.) are based on three independent experiments; $^{**}P<0.005$; $^{*}P<0.05$. (D) Quantitative results of matrix degradation shown in B. Data are expressed as the percentage relative to the level in control SrcY527F-transformed NIH3T3 cells, which was defined as 100%. Values (means ± s.d.) are based on at least three independent experiments; $^{**}P<0.005$; $^{*}P<0.05$. (E) The cells as in A were subjected to the Matrigel invasion assay in the presence (+) or absence (−) of 25 μM SP600125. Data are expressed as the percentage relative to the level in control SrcY527F-transformed NIH3T3 cells, which was defined as 100%. Values (means ± s.d.) are based on at least three independent experiments; $^{**}P<0.005$. (F) GFP, GFP-JNK1 and GFP-JNK2 were transiently expressed in SrcY527F-transformed NIH3T3 cells whose endogenous JNK1 or JNK2 had been suppressed by shRNAs specific to JNK1 (shJNK1) or JNK2 (shJNK2). The cells expressing shRNA specific to luciferase (shLuc) were used as the control. Equal amounts of whole-cell lysate were analyzed by immunoblotting with the indicated antibodies. The positions of GFP-JNK1, GFP-JNK2, endogenous JNK1 (endo-JNK1) and endogenous JNK2 (endo-JNK2) are indicated by arrows. WT, wild type; T183A/Y185F, kinase-deficient mutant. (G) The cells as in F were grown on fibronectin-coated glass coverslips for 24 hours and then stained for F-actin. The percentage of cells containing podosome rosettes in the total number of counted cells expressing GFP or GFP-JNK was determined ($n \geq 100$). Values (means ± s.d.) are based on three independent experiments. $^{**}P<0.005$; $^{*}P<0.05$.

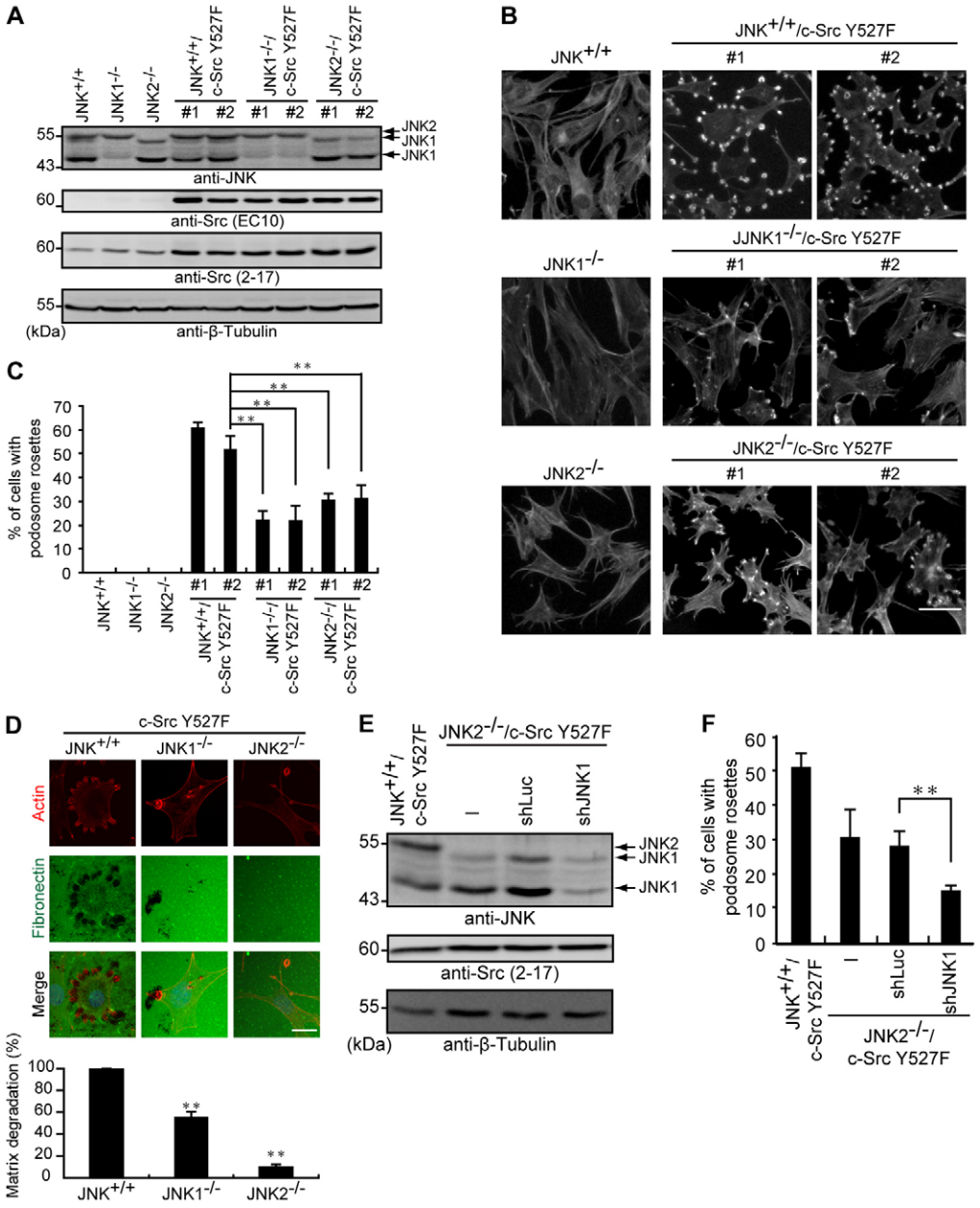

Fig. 3. SrcY527F is less able to induce podosome rosettes in JNK1$^{-/-}$ MEFs and JNK2$^{-/-}$ MEFs than in JNK$^{+/+}$ MEFs. (A) Equal amounts of whole-cell lysates from JNK$^{+/+}$ MEFs, JNK1$^{-/-}$ MEFs, JNK2$^{-/-}$ MEFs and MEFs transformed with chicken Src Y527F (two independent clones, #1 and #2, for each cell line) was analyzed by immunoblotting with the indicated antibodies (B) The cells as in panel A were grown on fibronectin-coated glass coverslips for 24 hours and then stained for F-actin. Scale bar: 50 μm. (C) Quantitative results of podosome rosette formation shown in B. The percentage of cells containing podosome rosettes in the total number of counted cells was determined ($n \geq 200$). Values (means ± s.d.) are based on three independent experiments; $^{**}P<0.005$. (D) SrcY527F-transformed JNK$^{+/+}$ MEFs, JNK1$^{-/-}$ MEFs and JNK2$^{-/-}$ MEFs were grown on glass coverslips coated with Alexa-Fluor-488-conjugated fibronectin for 12 hours. The cells were fixed and stained for F-actin. The degraded areas from total 10 random fields were measured and expressed as the percentage relative to the level in SrcY527F-transformed JNK$^{+/+}$ MEFs, which was defined as 100%. Values (means ± s.d.) are based on three independent experiments; $^{**}P<0.005$. Scale bar: 20 μm. (E) JNK1 was further depleted in SrcY527F-transformed JNK2$^{-/-}$ MEFs. SrcY527-transformed JNK2$^{-/-}$ MEFs (JNK2$^{-/-}$/Src Y527F) were infected with lentiviruses encoding shRNAs specific to JNK1 (shJNK1) or luciferase (shLuc). Equal amounts of whole-cell lysates were analyzed by immunoblotting with the indicated antibodies. (F) The cells as in panel E were grown on fibronectin-coated glass coverslips for 24 hours and then stained for F-actin. The percentage of cells containing podosome rosettes in the total number of counted cells was determined ($n \geq 200$). Values (means ± s.d.) are based on three independent experiments. $^{**}P<0.005$.

essential for podosome rosette formation. The suppression of podosome rosette formation by SP600125 was correlated with a decrease in matrix degradation (Fig. 1C).

To further examine the role of JNK in podosome rosette formation, JNK1 or JNK2 was depleted using short-hairpin RNAs (shRNAs) in SrcY527F-transformed NIH3T3 fibroblasts

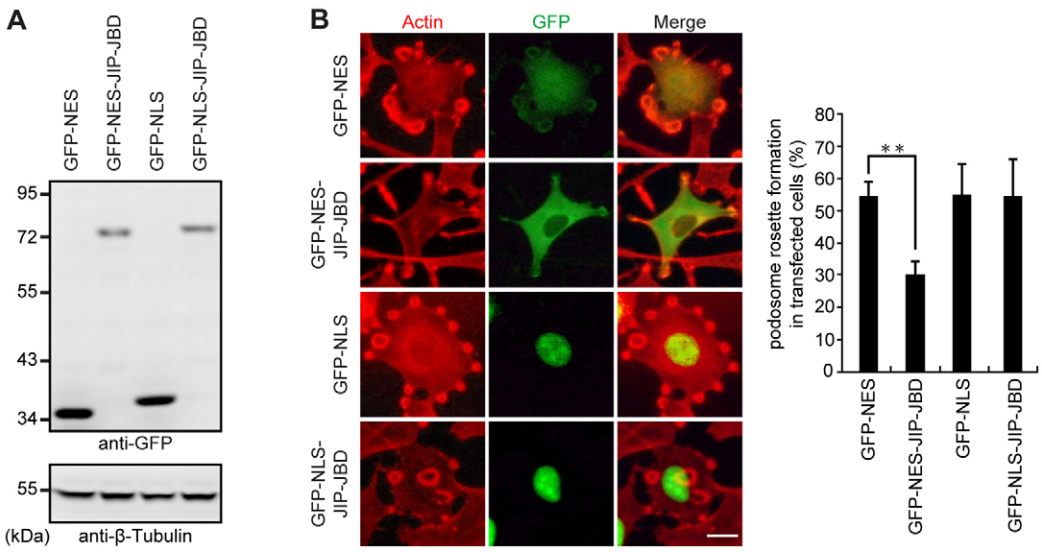

Fig. 4. Cytoplasmic JNK rather than nuclear JNK regulates podosome rosette formation. (A) The JNK-binding domain (JBD) of JNK-interacting protein (JIP) that serves as an inhibitor for JNK was fused with GFP-NES (nuclear export signal) or GFP-NLS (nuclear localization signal) to differentially inhibit JNK in the cytoplasm or nucleus. GFP-NES-JIP-JBD, GFP-NLS-JIP-JBD, GFP-NES and GFP-NLS were transiently expressed in SrcY527F-transformed NIH3T3 cells. Equal amounts of whole-cell lysates were analyzed by immunoblotting with the indicated antibodies. (B) Cells as in A were plated on fibronectin-coated glass coverslips for 24 hours and then stained for F-actin. The percentage of cells containing podosome rosettes in the total number of counted cells expressing GFP-tagged proteins was determined ($n \geq 100$). Values (means ± s.d.) are based on three independent experiments; $^{**}P < 0.005$. Scale bar: 20 μm.

(Fig. 2A). The depletion of JNK1 or JNK2 suppressed the formation of podosome rosettes (Fig. 2B,C), accompanied by decreases in matrix degradation (Fig. 2D) and invasion (Fig. 2E). In addition, the suppression of podosome rosette formation was partially restored by the expression of green fluorescent protein (GFP)-fused human JNK1 or JNK2 but not by the kinase-deficient (T183A/Y185F) mutant (Fig. 2F,G). These results, taken together, indicate that both JNK1 and JNK2 are important for podosome rosette formation in Src-transformed fibroblasts.

Podosomes can serve as the structural unit for superstructures such as podosome rosettes or belts. We noted that the Src-transformed fibroblasts with podosome rosettes had fewer podosome dots than the cells without podosome rosettes (supplementary material Fig. S1B and Fig. S2A). The suppression of podosome rosette formation by the JNK depletion increased the number of podosome dots in SrcY527F-transformed NIH3T3 fibroblasts (supplementary material Fig. S2B,C), suggesting that the prevention of podosome rosette assembly keeps podosomes as dot-like structures. In addition, Jun kinases have been reported to regulate the expression of MMPs (Manning and Davis, 2003). Indeed, we found that the depletion of JNK1 decreased the expression of MT1-MMP1 in SrcY527F-transformed NIH3T3 fibroblasts (supplementary material Fig. S3).

To examine the necessity of JNK1 and JNK2 in the formation of podosome rosettes, JNK1-null ($JNK1^{-/-}$) mouse embryo fibroblasts (MEFs), JNK2-null ($JNK2^{-/-}$) MEFs and their wild-type (WT) counterparts ($JNK^{+/+}$) were used in this study (Fig. 3). Prior to transformation by the SrcY527F mutant, $JNK^{+/+}$, $JNK1^{-/-}$ and $JNK2^{-/-}$ MEFs had no podosomes. The Src Y527F mutant potently induced podosome rosettes in $JNK^{+/+}$ MEFs (Fig. 3A–C). However, podosome rosettes induced by SrcY527F were much fewer in $JNK1^{-/-}$ MEFs and $JNK2^{-/-}$ MEFs compared with $JNK^{+/+}$ MEFs (Fig. 3A–C). In addition, the podosome rosettes in SrcY527F-transformed $JNK2^{-/-}$ MEFs were less potent at degrading matrix (Fig. 3D). Knockdown of JNK1 further decreased the formation of podosome rosettes in Src-transformed $JNK2^{-/-}$ MEFs (Fig. 3E,F). These results indicate that both JNK1 and JNK2 contribute to podosome rosette formation, but neither protein can compensate for the function of the other in this process.

Cytoplasmic JNK rather than nuclear JNK promotes the formation of podosome rosettes

Active JNK proteins are present in both the nucleus and cytoplasm. Most of the known JNK functions are mediated by nuclear JNK, which activates transcriptional factors such as AP1, ultimately regulating gene expression (Manning and Davis, 2003). However, JNK also acts in the cytoplasm. For example, JNK phosphorylates paxillin at focal adhesions and promotes cell migration (Huang et al., 2003). To examine whether the stimulatory effect of JNK on podosome rosette formation is mediated by cytoplasmic or nuclear JNK, the JNK-binding domain (JBD) of JNK-interacting protein (JIP), which serves as a JNK inhibitor (Björkblom et al., 2005), was fused with GFP-NES (nuclear export signal) or GFP-NLS (nuclear localization signal) to differentially inhibit JNK in the cytoplasm or nucleus, respectively. Only when expressed in the cytoplasm did JIP-JBD inhibit podosome rosette formation (Fig. 4). These data suggest that cytoplasmic JNK rather than nuclear JNK is involved in the formation of podosome rosettes.

The kinase activity of JNK is not required for the localization of JNK at podosome rosettes

Our results indicate that the catalytic activity of JNK is essential for its function to promote podosome rosette formation (Fig. 1B and Fig. 2G). However, we found that FLAG-tagged JNK1/JNK2 and their kinase-deficient (T183A/Y185F) mutants localized to

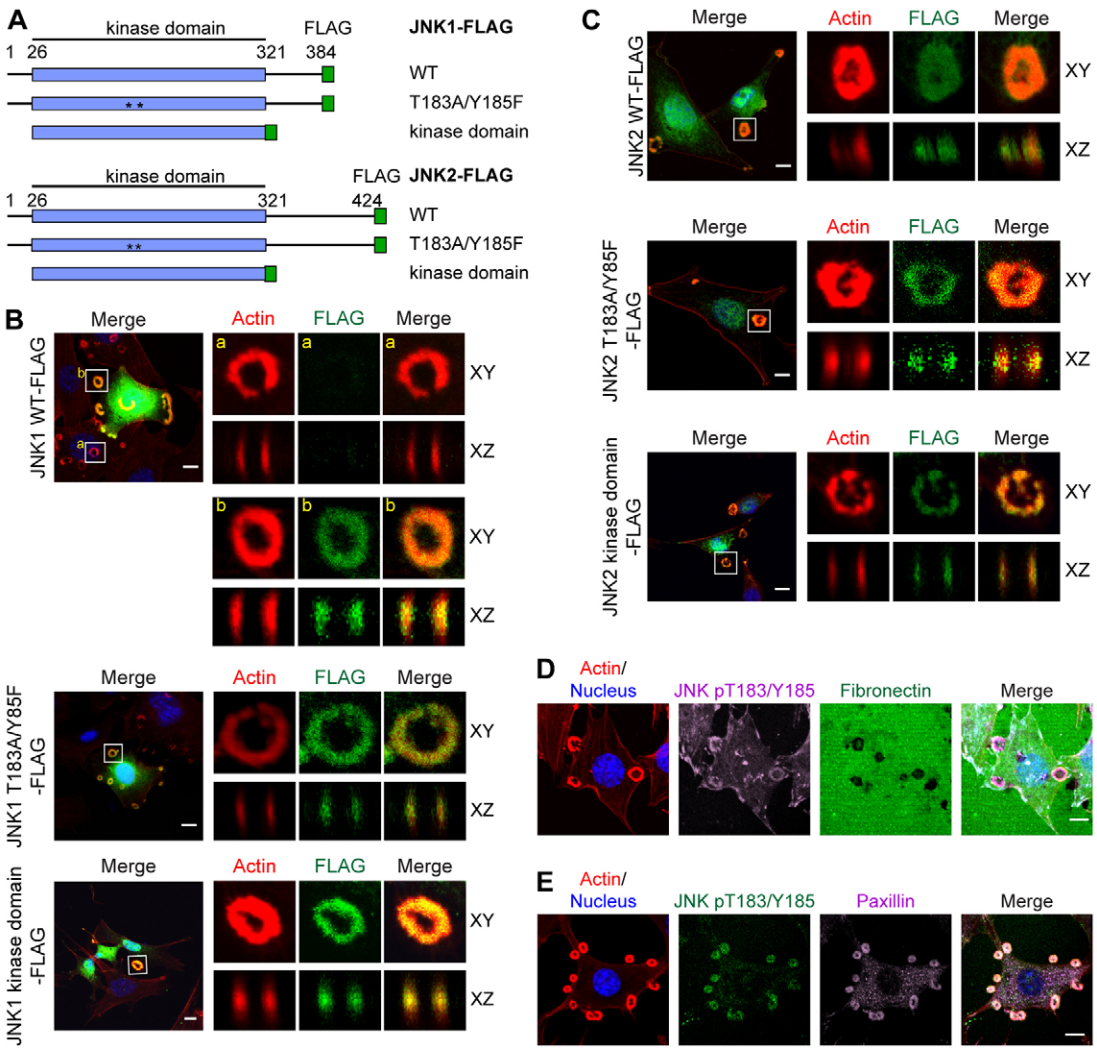

Fig. 5. The kinase activity of Jun kinases is not required for their localization at podosome rosettes. (A) Schematic presentation of FLAG-JNK1, FLAG-JNK2 and their mutants. The kinase domain contains aa 26–321. WT, wild type; T183A/Y185F, the kinase-deficient mutant. (B) FLAG-JNK1 and mutants were transiently expressed in SrcY527F-transformed NIH3T3 cells. The cells were fixed and then stained for F-actin, FLAG-JNK and nuclei. *Z*-stack images were obtained and reconstructed. *XY* and *XZ* sections of the boxed region containing a podosome rosette are enlarged. Box (a) contains a podosome rosette from the cell without the expression of FLAG-JNK. Box (b) contains a podosome rosette from the cell with the expression of FLAG-JNK. (C) FLAG-JNK2 and mutants were transiently expressed in SrcY527F-transformed NIH3T3 cells. The cells were fixed and then stained for F-actin, FLAG-JNK and nuclei. (D) SrcY527F-transformed NIH3T3 cells were grown on Alexa-Fluor-488-conjugated fibronectin for 12 hours. The cells were fixed and then stained for F-actin, active JNK (JNK pT183/Y185) and nuclei. (E) SrcY527F-transformed NIH3T3 cells were grown on fibronectin for 12 hours. The cells were fixed and then stained for F-actin, active JNK (JNK pT183/Y185), paxillin and nuclei. Scale bars: 10 μm.

podosome rosettes (Fig. 5A–C), indicating that the catalytic activity of JNK is not required for JNK localization to podosome rosettes. In addition, the kinase domain per se was able to localize to podosome rosettes (Fig. 5A–C), indicating that the kinase domain of JNK is responsible for its localization to podosome rosettes. The active (pT183/Y185) JNK proteins were detected at podosome rosettes where they colocalized with paxillin (Fig. 5D,E).

Paxillin does not mediate the effect of JNK on podosome rosette formation

Paxillin is a crucial component of podosomes and is phosphorylated by JNK at Ser178 (Huang et al., 2003). To examine whether paxillin is the downstream effector for JNK to promote podosome rosette formation, Ser178 phosphorylation of paxillin was analyzed. Ser178 phosphorylation of paxillin was not detected in SrcY527F-transformed NIH3T3 fibroblasts (Fig. 6A). In addition, the suppression of podosome rosette formation by knockdown of paxillin was rescued by GFP-paxillin and its Ser178 mutants in SrcY527F-transformed NIH3T3 fibroblasts (Fig. 6B,C). The paxillin S178A and S718D mutants localized to podosome rosettes (Fig. 6D) and did not affect the matrix degradation activity of podosome rosettes (Fig. 6E). The phosphorylation of paxillin at Tyr118 by Src has been shown to be important for the role of paxillin in podosome formation (Badowski et al., 2008). We found that mutation of paxillin at Ser178 did not affect Tyr118 phosphorylation in SrcY527F-transformed NIH3T3 fibroblasts (Fig. 6F). Together, these results

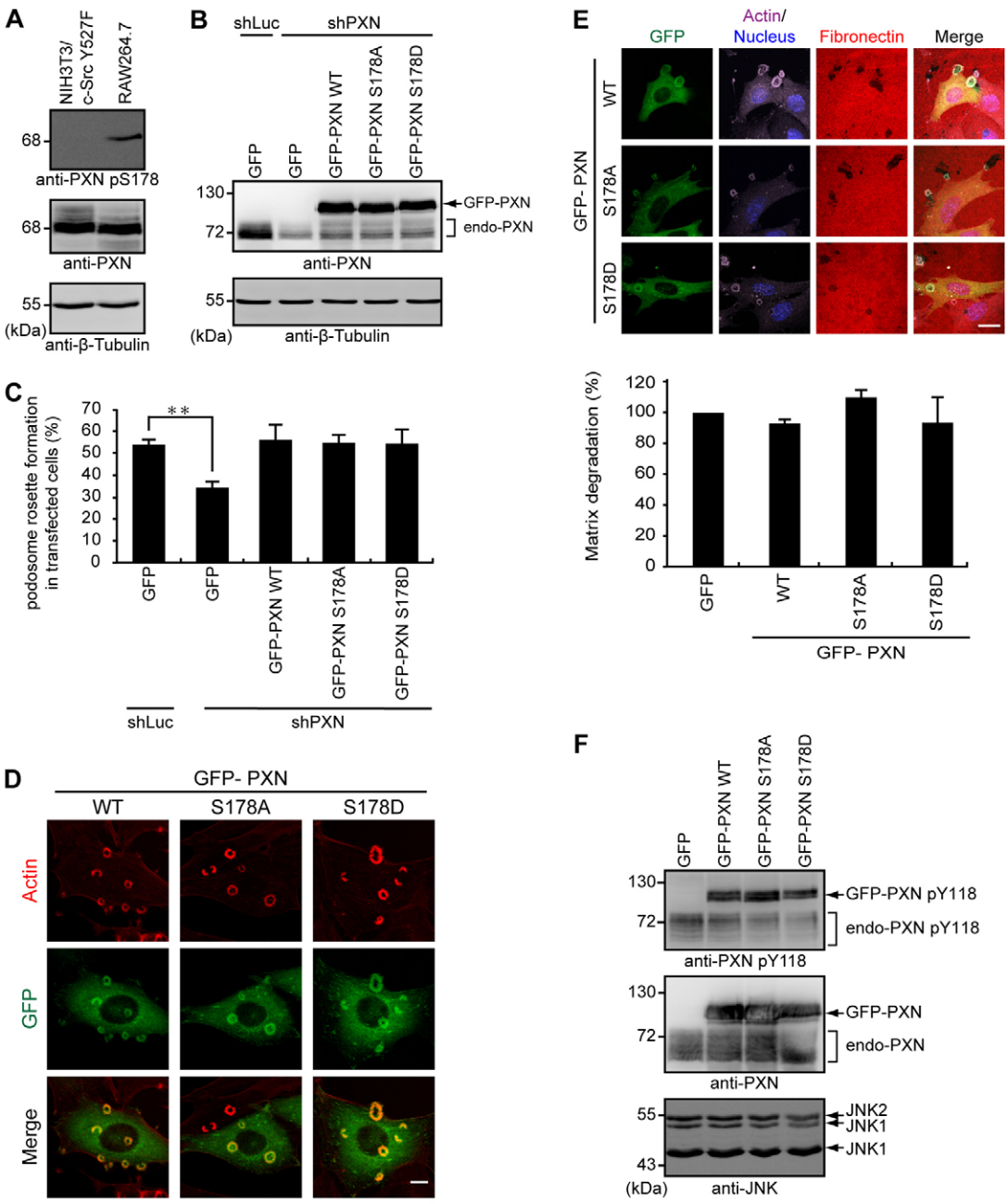

Fig. 6. Paxillin does not mediate the effect of JNK on promoting podosome rosette formation in SrcY527F-transformed NIH3T3 fibroblasts. (A) An equal amount of whole cell lysates from SrcY527F-transformed NIH3T3 cells and mouse RAW264.7 cells was analyzed by immunoblotting with the indicated antibodies. PXN, paxillin. (B) GFP, GFP-paxillin (GFP-PXN) and its S178 mutants were transiently expressed in SrcY527F-transformed NIH3T3 cells expressing shRNAs specific to paxillin (shPXN) or luciferase (shLuc) as a control. An equal amount of whole cell lysates was analyzed by immunoblotting with the indicated antibodies. The positions of endogenous paxillin (endo-PXN) and GFP-paxillin (GFP-PXN) are indicated. (C) The cells as in panel B were plated on fibronectin-coated glass coverslips for 24 hours and then stained for F-actin. The percentage of cells containing podosome rosettes in the total number of counted cells expressing GFP or GFP-paxillin was determined ($n \geq 100$). Values (means ± s.d.) are based on three independent experiments; $^{**}P < 0.005$. (D) The mutation at S178 does not affect the localization of GFP-paxillin at podosome rosettes. GFP-paxillin (GFP-PXN) WT, S178A and S178D were transiently expressed in SrcY527F-transformed NIH3T3 cells. The cells were plated on fibronectin-coated glass coverslips and then stained for F-actin. (E) SrcY527F-transformed NIH3T3 cells transiently expressing GFP, GFP-paxillin (GFP-PXN) WT, S178A or S178D were grown on glass coverslips coated with Alexa-Fluor-546-conjugated fibronectin for 12 hours. The cells were fixed and stained for actin with anti-β actin antibody. The degraded areas from 25 counted cells expressing GFP or GFP-paxillin (GFP-PXN) were measured and expressed as the percentage relative to the level in the cells expressing GFP, which was defined as 100%. Values (means ± s.d.) are based on three independent experiments. (F) Equal amounts of whole-cell lysates from SrcY527F-transformed NIH3T3 cells expressing GFP or GFP-paxillin were analyzed by immunoblotting with the indicated antibodies. The positions of endogenous paxillin (endo-PXN), GFP-paxillin (GFP-PXN) and Tyr118 phosphorylation of paxillin (endo-PXN pY118 and GFP-PXN pY118) are indicated by arrows. Scale bars: 10 μm (D), 20 μm (E).

indicate that the effect of JNK on the promotion of podosome rosette formation is not mediated by paxillin.

Phosphorylation of moesin at Thr558 by JNK is important for podosome rosette formation

In our efforts to identify the JNK substrate with an important role in podosome rosettes, moesin, a member of the ERM (for ezrin, radixin and moesin) protein family, was identified as a JNK substrate. We found that the phosphorylation of moesin at Thr558 was inhibited by the JNK inhibitor SP600125 or JNK shRNAs in SrcY527F-transformed NIH3T3 cells (Fig. 7A,B). Thr558 phosphorylation was enhanced by the overexpression of GFP-JNK1 and GFP-JNK2 but not their kinase-deficient mutants in Src-transformed NIH3T3 fibroblasts (Fig. 7C). *In vitro*, JNK1 and JNK2 directly phosphorylated moesin but not its T558A mutant (Fig. 7D,E). JNK and ERM proteins colocalized at

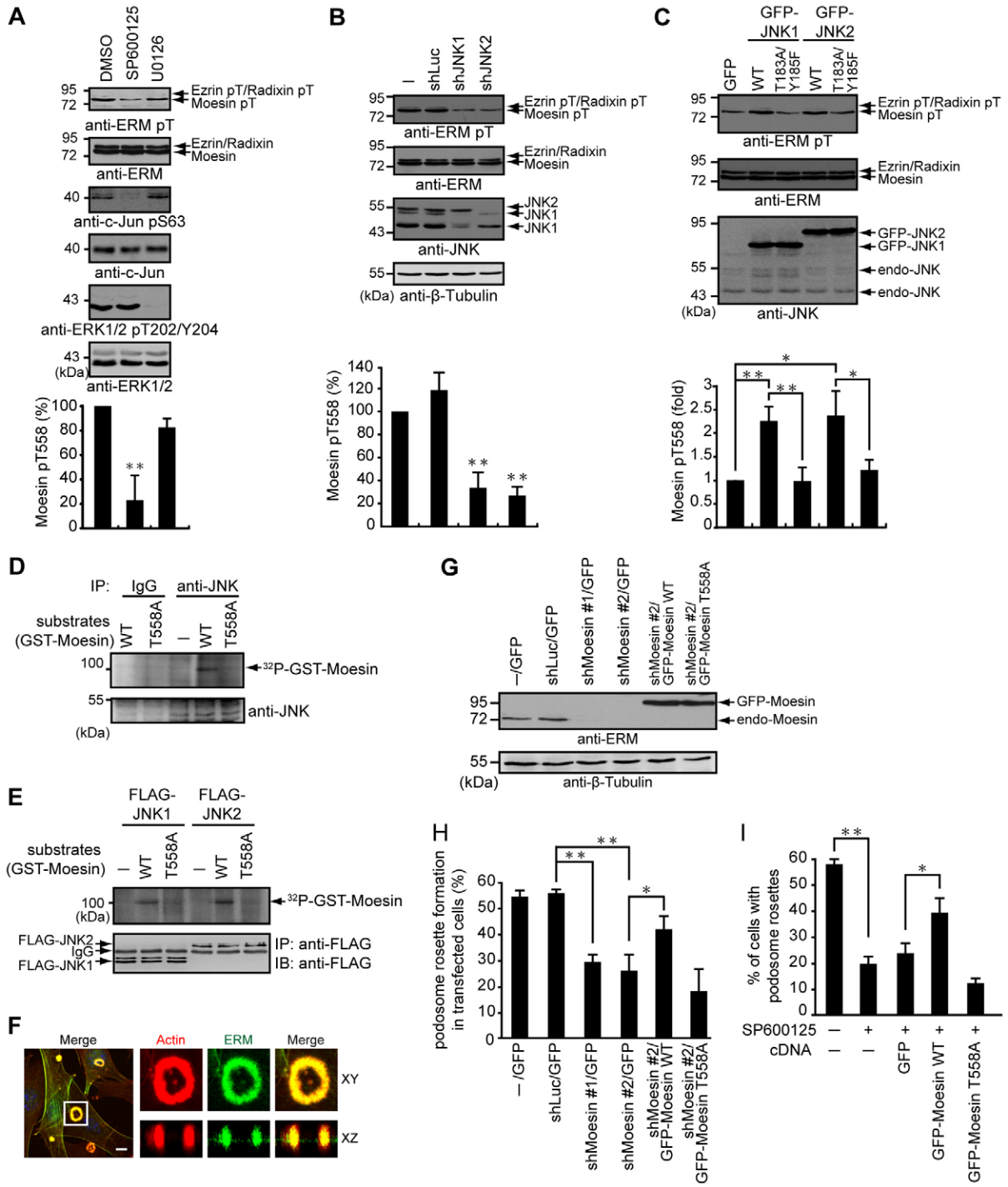

Fig. 7. See next page for legend.

podosome rosettes (Fig. 7F). To examine the role of moesin in podosome rosette formation, moesin was depleted by shRNAs in SrcY527F-transformed NIH3T3 fibroblasts. The depletion of moesin suppressed the formation of podosome rosettes, which was partially restored by the expression of GFP-moesin but not its T558A mutant (Fig. 7G,H). The overexpression of GFP-moesin, but not its T558A mutant, counteracted the inhibitory effect of the JNK inhibitor SP600125 on podosome rosette formation (Fig. 7I). Taken together, our results suggest that JNK facilitates the formation of podosome rosettes by phosphorylating moesin at Thr558.

Fig. 7. JNK promotes the formation of podosome rosettes by phosphorylating moesin in SrcY527F-transformed NIH3T3 fibroblasts. (A) SrcY527F-transformed NIH3T3 cells were treated with 25 μM SP600125 (a JNK inhibitor) or 5 μM U0126 (a MEK1 inhibitor) for 3 hours. For the control, an equal volume of the solvent DMSO was added to the medium. Equal amounts of whole-cell lysates were analyzed by immunoblotting with the indicated antibodies. The pT558 phosphorylation of moesin was quantified and expressed as the percentage relative to the level in DMSO-treated cells, which was defined as 100%. Values (means ± s.d.) are based on three independent experiments; $^{**}P<0.005$. (B) Equal amounts of whole-cell lysates from SrcY527F-transformed NIH3T3 cells expressing shRNAs specific to JNK1 (shJNK1), JNK2 (shJNK2) or luciferase (shLuc; as a control) were analyzed by immunoblotting with the indicated antibodies. pT558 phosphorylation of moesin was quantified and expressed as the percentage relative to the level in control SrcY527F-transformed NIH3T3 cells, which was defined as 100%. Values (means ± s.d.) are based on three independent experiments; $^{**}P<0.005$. (C) GFP, GFP-JNK and the T183A/Y185F mutant were transiently expressed in SrcY527F-transformed NIH3T3 cells. An equal amount of whole-cell lysates was analyzed by immunoblotting with the indicated antibodies. The pT558 phosphorylation of moesin was quantified and expressed as fold relative to the level of SrcY527F-transformed NIH3T3 cells expressing GFP. Values (means ± s.d.) are based on three independent experiments; $^{**}P<0.005$; $^{*}P<0.05$. (D) Endogenous JNK proteins from SrcY527F-transformed NIH3T3 cells were immunoprecipitated (IP) by anti-JNK or a control immunoglobulin G (IgG). The immunocomplexes were subjected to immunoblotting with anti-JNK or to an *in vitro* kinase assay using purified GST-moesin or its T558A mutant as the substrate. ^{32}P-labeled GST-moesin was visualized by autoradiography. (E) FLAG-JNK1 and FLAG-JNK2 were transiently expressed in HEK293 cells. FLAG-JNK proteins were immunoprecipitated (IP) with anti-FLAG and the immunocomplexes were subjected to immunoblotting (IB) with anti-FLAG or to an *in vitro* kinase assay using purified GST-moesin or its T558A mutant as the substrate. ^{32}P-labeled GST-moesin was visualized by autoradiography. (F) SrcY527F-transformed NIH3T3 cells were grown on fibronectin-coated coverslips. The cells were fixed and then stained for F-actin and ERM proteins. *Z*-stack images were obtained and reconstructed. *XY* and *XZ* sections of the white box containing a podosome rosette are enlarged. Scale bar: 10 μm. (G) GFP, GFP-moesin and the T558A mutant were transiently expressed in SrcY527F-transformed NIH3T3 cells that stably expressed shRNAs specific to moesin (shMeosin, clone #1 and #2) or luciferase (shLuc). Equal amounts of whole-cell lysates were analyzed by immunoblotting with the indicated antibodies. The positions of endogenous moesin (endo-Moesin) and GFP-Moesin are indicated by arrows. (H) Cells as in G were grown on fibronectin-coated glass coverslips for 24 hours and then stained for F-actin. The percentage of cells containing podosome rosettes in the total number of counted cells expressing GFP or GFP-moesin was determined ($n\geq100$). Values (means ± s.d.) are based on three independent experiments; $^{**}P<0.005$; $^{*}P<0.05$. (I) GFP, GFP-moesin and GFP-moesin T558A were transiently expressed in SrcY527F-transformed NIH3T3 cells for 24 hours. The cells were plated on fibronectin-coated glass coverslips for 21 hours and then treated with 25 μM SP600125 (+) or DMSO (−) for 3 hours. The cells were fixed and then stained for F-actin. The percentage of cells containing podosome rosettes in the total number of counted cells expressing GFP or GFP-moesin was determined ($n\geq100$). Values (means ± s.d.) are based on three independent experiments. $^{**}P<0.005$; $^{*}P<0.05$.

Discussion

In this study, we demonstrated that the phosphorylation of moesin at Thr558 by JNK is important for podosome rosette formation in SrcY527F-transformed NIH3T3 fibroblasts. Paxillin was shown to be phosphorylated by JNK and important for focal adhesion turnover in breast cancer MDA-MB-231 cells (Huang et al., 2003); however, this is not the case for podosome rosette formation in SrcY527F-transformed NIH3T3 fibroblasts. In addition, we excluded the involvement of JIP1 in podosome rosette formation in SrcY527F-transformed NIH3T3 fibroblasts (supplementary material Fig. S4). However, it is not clear whether other JIP proteins (in particular, JIP3) are involved in podosome rosette formation. JIP3 has been shown to form a complex with focal adhesion kinase (FAK) and to function as a scaffold for the JNK signaling pathway and a regulator of cell migration in response to fibronectin (Takino et al., 2005). We previously demonstrated that FAK is required for the assembly of podosome rosettes (Pan et al., 2011). Experiments to examine the potential connection of JIP3, FAK and JNK in podosome rosette formation are currently in progress.

Moesin is phosphorylated at Thr558 by Rho-associated kinase II (ROCK II) (Matsui et al., 1998; Oshiro et al., 1998) and lymphocyte-oriented kinase (LOK) (Belkina et al., 2009). LOK is predominantly expressed in lymphocytes; therefore, LOK is less likely to phosphorylate ERM proteins and to regulate podosome rosette formation in non-hematopoietic cells. We previously reported that the Rho–ROCK-II signaling axis plays a negative role in the formation of podosome rosettes in Src-transformed fibroblasts and other types of cells (Pan et al., 2011; Pan et al., 2013). To facilitate podosome rosette formation, Rho and/or ROCK II are often found to be repressed in cells. For example, active Src represses the Rho–ROCK pathway by activating RhoGAP (Arthur et al., 2000; Roof et al., 2000) or directly phosphorylating and inhibiting ROCK II (Lee et al., 2010; Pan et al., 2013).

ERM proteins crosslink the actin cytoskeleton to several transmembrane proteins that include CD44 (Tsukita et al., 1994; Legg and Isacke, 1998), the Na^+/H^+-exchanger NHE1 (Denker et al., 2000), CD43 (Serrador et al., 1998) and intercellular adhesion molecules (ICAMs) (Heiska et al., 1998; Serrador et al., 1997; Yonemura et al., 1998). Among these transmembrane proteins, the hyaluronan receptor CD44 has been reported to be important for podosome belt formation in osteoclasts (Chabadel et al., 2007). In addition, the recruitment of the Na^+/H^+-exchanger NHE1 to invadopodia is necessary for the invasiveness of cancer cells (Busco et al., 2010; Magalhaes et al., 2011). In this study, we demonstrated that JNK phosphorylates moesin at Thr558, which could activate moesin and induce binding to CD44 and/or NHE1. The crosslinking of CD44 to the actin filaments mediated by moesin might recruit CD44 to podosomes and could further facilitate the initial assembly and/or maintenance of podosome rosettes.

In addition to its function as a receptor for hyalunonan and other components of the extracellular matrix, CD44 can act as a specialized ‘platform’ for the localization of several growth factors and MMPs on the cell surface (Yu and Stamenkovic, 2000; Yu et al., 2002). Specifically, MMP7 and MMP9 are recruited to the cell surface by CD44 (Yu and Stamenkovic, 1999; Yu et al., 2002). In addition, CD44 has also been reported to

interact with Src and to promote cortactin-mediated cytoskeletal function (Bourguignon et al., 2001). Both Src and cortactin are essential components of podosomes (Tehrani et al., 2006; Destaing et al., 2008). All of these previous studies support the potential significance of CD44 in the structure and activity of podosomes; however, further studies are needed to characterize the role of CD44 in podosomes. Furthermore, the interactions between CD44 and ERM proteins are important for tumor formation as well as several aspects of the immune system, hematopoiesis and bacterial infection (Ponta et al., 2003); therefore, our findings regarding the phosphorylation of moesin by JNK implicate a widespread influence of JNK on these processes.

Materials and Methods

Materials

Polyclonal anti-cortactin (H-191), anti-ERK1 (K-23), anti-JNK (FL), anti-Jun (N) and anti-MT1-MMP (L-15) antibodies, and monoclonal anti-GFP, anti-JIP-1 (B-7) and anti-β-tubulin (D-10) antibodies were purchased from Santa Cruz Biotechnology (Santa Cruz, CA). Polyclonal anti-ERK1/2 pT202/Y204, anti-ERM, anti-ERM pT (ezrin pT567/radixin pT564/moesin pT558), anti-JNK pT183/Y185 (81E11) and anti-Jun pS63 antibodies were purchased from Cell Signaling Technology (Beverly, MA). Monoclonal anti-paxillin and Matrigel were purchased from BD Transduction Laboratories (San Jose, CA). Monoclonal anti-FLAG (M2) antibody, DMSO, U0126 and protein-A–Sepharose beads were purchased from Sigma-Aldrich (St Louis, MO). Polyclonal anti-paxillin pS178 and anti-paxillin pY118 antibodies, blasticidin, Dulbecco's modified Eagle's medium (DMEM) and Lipofectamine were purchased from Life Technologies-Invitrogen (Carlsbad, CA). Polyclonal anti-MMP9 antibody, monoclonal anti-MMP2 and anti-Src (EC10 for detecting chicken Src) antibodies, SP600125, PD98059, fibronectin and puromycin were purchased from EMD Millipore (Billerica, MA). Glutathione Sepharose 4B beads were purchased from GE Healthcare. Mouse ascites containing the monoclonal anti-Src (2–17 for detecting total Src proteins) antibody produced by hybridoma (CRL-2651) were prepared in our laboratory.

Plasmids

Human cDNAs encoding JNK1α1 and JNK2α2 were provided by Dr Zigang Dong (Hormel Institute, University of Minnesota, MN) and have been described previously (Yao et al., 2007). The pEGFP-NES-JIP-JBD (aa 1~277) and pEGFP-NLS-JIP-JBD (aa 1~277) plasmids were provided by Dr Eleanor Coffey (Åbo Akademi and Turku University, Finland) and have been previously described (Björkblom et al., 2005). The pEGFP-paxillin plasmid was provided by Dr Zee-Fen Chang (National Yang-Ming University, Taiwan). The following plasmids were constructed in our laboratory: pEGFP-JNK1α1 WT and T183A/Y185F; pEGFP-JNK2α2 WT and T183A/Y185F; pCMV-3Tag-3A-JNK1α1 WT, T183A/Y185F and the kinase domain (aa 26~321); pCMV-3Tag-3A-JNK2α2 WT, T183A/Y185F and the kinase domain (aa 26~321); pEGFP-moesin WT, T558A and a shRNA-resistant mutant (nt. C820T/T822A/C823A); pGEX-moesin WT and T558A; pEGFP-paxillin WT, S178A and S178D. All mutagenesis was performed using a QuikChange site-directed mutagenesis kit (Stratagene, La Jolla, CA) and the desired mutations were confirmed by dideoxy DNA sequencing.

Cell culture and transfections

SrcY527F-transformed NIH3T3 fibroblasts were previously described (Pan et al., 2011). For transient expression, SrcY527F-transformed NIH3T3 fibroblasts were transfected with plasmids using LipofectAMINE. $JNK^{+/+}$ MEFs, $JNK1^{-/-}$ MEFs and $JNK2^{-/-}$ MEFs were kindly provided by Dr Zigang Dong and have been previously described (Yao et al., 2007). To generate SrcY527-transformed MEFs, MEFs were co-transfected with 3 μg of pEVX-SrcY527F and 0.3 μg of pEF6/V5-His-TOPO (Invitrogen) by LipofectAMINE following the manufacturer's instructions. The cells were selected in medium containing 10 μg/ml blasticidin. After 10 days, the blasticidin-resistant cells were expanded for analysis.

Lentivirus production and infection

The lentiviral expression system for shRNA was provided by the National RNAi Core Facility, Academia Sinica, Taiwan. For small-hairpin RNA (shRNA)-mediated knockdown, the pLKO-AS1.puro plasmids encoding shRNAs were obtained from the National RNAi Core Facility. The target sequences for JNK1 are 5′-GTCTGTCAATGACATGTCTT-3′ (#1) and 5′-CGGGACTTAAAGCCTAGT-AAT-3′ (#2). The target sequences for JNK2 are 5′-CTACTCCTTCTCAGTCGT-CAT-3′ (#1) and 5′-CAGACCAAAGTACCCTGGAAT-3′ (#2). The target sequences for moesin are 5′-CCAGTTGGAAATGGCTCGAAA-3′ (#1) and 5′-GCTTCGGATTAACAAGCGGAT-3′ (#2). The target sequences for JIP1 are 5′-GCAGATGCAGTTTATTGTAAT-3′ (#1) and 5′-CACGCTGAATAATAACTC-TTT-3′ (#2). The target sequence for paxillin is 5′-TCTGAACTTGACCG-GCTGTTA-3′. To produce lentiviruses, HEK293T cells were co-transfected with 2.25 μg pCMV-ΔR8.91, 0.25 μg pMD.G and 2.5 μg pLKO-AS1.puro-shRNA using LipofectAMINE. After 3 days, the medium containing lentivirus particles was collected and stored at −80℃. The cells were infected with recombinant lentiviruses in the presence of 8 μg/ml polybrene (Sigma-Aldrich) for 24 hours. Subsequently, the cells were selected in growth medium containing 2–2.5 μg/ml puromycin for 3 days, and puromycin-resistant cells were collected for analysis.

Immunoprecipitation and immunoblotting

To prepare whole cell lysates, cells were lysed in 1% Nonidet P-40 lysis buffer (1% Nonidet P-40, 20 mM Tris-HCl, pH 8.0, 137 mM NaCl, 10% glycerol and 1 mM Na_3VO_4) containing protease inhibitors (phenylmethylsulfonyl fluoride, aprotinin and leupeptin). To collect conditioned medium, 8×10^5 cells were grown on a 6 cm dish in growth medium for 12 hours and then incubated in 4 ml serum-free medium for another 14 hours. The conditioned medium was collected and concentrated by centrifugation using an Ultracel 30 K (EMD Millipore). An equal amount of whole-cell lysates or conditioned medium was separated by SDS-PAGE. Immunoblotting and immunoprecipitation were performed as previously described (Chen and Chen, 2006). Chemiluminescent signals were detected and quantified using a luminescence image system (LAS-3000, Fujifilm).

In vitro kinase assay

FLAG-JNK1 and FLAG-JNK2 were transiently expressed in HEK293 cells. After 36 hours, the cells were lysed with 1% Nonidet P-40 lysis buffer containing protease inhibitors and then the cell lysates were incubated with 0.2 μg of monoclonal anti-FLAG antibody for 1.5 hours at 4℃. Immunocomplexes were immobilized on protein-A–Sepharose beads and washed three times with 1% Nonidet P-40 lysis buffer and twice with 50 mM Tris-HCl, pH 7.4. Kinase reactions were conducted in 40 μl of kinase buffer (50 mM HEPES, pH 7.4, 25 mM $MgCl_2$) containing 10 μCi of [γ-^{32}P]ATP and 0.25 μg of GST-moesin WT or T558A for 30 minutes at 25℃. The reaction was terminated by SDS sample buffer and the proteins were fractionated by SDS-PAGE. The ^{32}P-labeled proteins were visualized by autoradiography.

Matrix degradation assay

The matrix degradation assay was carried out as previously described (Pan et al., 2011). SrcY527-transformed NIH3T3 cells were seeded onto coverslips coated with Alexa-Fluor-546-fibronectin or Alexa-Fluor-488-fibronectin for 12 or 24 hours. The matrix degraded areas were determined using the Image-Pro Plus® software version 5.1. A total of ten random fields equivalent to 2 mm^2 were measured.

Matrigel invasion assay

Twenty-four-well Transwell chambers (Costar) with membranes with 8 μm pores were coated with 100 μl Matrigel (~0.4 mg/ml). The lower chamber was loaded with 750 μl growth medium. The cells were added to the upper chamber in 250 μl serum-free medium. After 24 hours, the cells that had migrated through the Matrigel were fixed by methanol, stained with Giemsa stain and counted.

Immunofluorescent staining and laser-scanning confocal fluorescent microscopy

For immunofluorescent staining, cells were fixed by 4% paraformaldehyde in phosphate-buffered saline (PBS) for 30 minutes at room temperature and permeabilized with 0.05% Triton X-100 in PBS for 10 minutes at room temperature. To stain FLAG-JNK, cells were fixed in PTEMF buffer (50 mM PIPES, pH 6.8, 0.2% Triton X-100, 10 mM EGTA, 1 mM $MgCl_2$, 3.7% paraformaldehyde and 0.25 mM $NaHCO_3$) for 30 minutes at room temperature and permeabilized with 0.1% Triton X-100 in PBS for 10 minutes at room temperature. The fixed cells were stained with primary antibodies at 4℃ overnight, followed by Rhodamine-conjugated or Cy5-conjugated secondary antibodies (Invitrogen) for 3 hours at room temperature. The primary antibodies used in immunofluorescent staining in this study were polyclonal anti-cortactin (1:200), polyclonal anti-ERM (1:100), polyclonal anti-JNK pT183/Y185 (1:100), monoclonal anti-paxillin (1:200) and monoclonal anti-FLAG (1:400). Rhodamine-conjugated phalloidin and Alexa-Fluor-488-conjugated phalloidin (Invitrogen) were used to stain actin filaments. Coverslips were mounted in anti-Fade DAPI-Fluoromount-G (Southern Biotech; Birmingham, AL) and viewed using a Zeiss LSM510 laser-scanning confocal microscope image system with a Zeiss 20× Plan-Apochromat (NA 0.6), a Zeiss 63× Plan-Apochromat (NA 1.2) or a Zeiss 100× Plan-Apochromat objective (NA 1.4, oil).

Statistics

Statistical analyses were carried out using the Student's *t*-test. Differences were considered to be statistically significant at $P<0.05$ or $P<0.005$.

Acknowledgements

We are grateful to Drs Zigang Dong, Eleanor Coffey and Zee-Fen Chang for providing reagents.

Author contributions

Y.-R.P. and H.-C.C. designed experiments and wrote the manuscript. Y.R.P., W.-S.T. and P.-W.C. performed experiments.

Funding

This work was supported by the National Science Council, Taiwan [grant number NSC100-2320-B-005-004-MY3]; by the National Health Research Institutes, Taiwan [grant number NHRI-EX101-10103BI]; and by the ATU plan from the Ministry of Education, Taiwan.

Supplementary material available online at
http://jcs.biologists.org/lookup/suppl/doi:10.1242/jcs.134361/-/DC1

References

Arpin, M., Chirivino, D., Naba, A. and Zwaenepoel, I. (2011). Emerging role for ERM proteins in cell adhesion and migration. *Cell Adh. Migr.* **5**, 199-206.

Arthur, W. T., Petch, L. A. and Burridge, K. (2000). Integrin engagement suppresses RhoA activity via a c-Src-dependent mechanism. *Curr. Biol.* **10**, 719-722.

Badowski, C., Pawlak, G., Grichine, A., Chabadel, A., Oddou, C., Jurdic, P., Pfaff, M., Albigès-Rizo, C. and Block, M. R. (2008). Paxillin phosphorylation controls invadopodia/podosomes spatiotemporal organization. *Mol. Biol. Cell* **19**, 633-645.

Belkina, N. V., Liu, Y., Hao, J. J., Karasuyama, H. and Shaw, S. (2009). LOK is a major ERM kinase in resting lymphocytes and regulates cytoskeletal rearrangement through ERM phosphorylation. *Proc. Natl. Acad. Sci. USA* **106**, 4707-4712.

Björkblom, B., Ostman, N., Hongisto, V., Komarovski, V., Filén, J. J., Nyman, T. A., Kallunki, T., Courtney, M. J. and Coffey, E. T. (2005). Constitutively active cytoplasmic c-Jun N-terminal kinase 1 is a dominant regulator of dendritic architecture: role of microtubule-associated protein 2 as an effector. *J. Neurosci.* **25**, 6350-6361.

Bogoyevitch, M. A. and Kobe, B. (2006). Uses for JNK: the many and varied substrates of the c-Jun N-terminal kinases. *Microbiol. Mol. Biol. Rev.* **70**, 1061-1095.

Bourguignon, L. Y., Zhu, H., Shao, L. and Chen, Y. W. (2001). CD44 interaction with c-Src kinase promotes cortactin-mediated cytoskeleton function and hyaluronic acid-dependent ovarian tumor cell migration. *J. Biol. Chem.* **276**, 7327-7336.

Brecht, S., Kirchhof, R., Chromik, A., Willesen, M., Nicolaus, T., Raivich, G., Wessig, J., Waetzig, V., Goetz, M., Claussen, M. et al. (2005). Specific pathophysiological functions of JNK isoforms in the brain. *Eur. J. Neurosci.* **21**, 363-377.

Busco, G., Cardone, R. A., Greco, M. R., Bellizzi, A., Colella, M., Antelmi, E., Mancini, M. T., Dell'Aquila, M. E., Casavola, V., Paradiso, A. et al. (2010). NHE1 promotes invadopodial ECM proteolysis through acidification of the peri-invadopodial space. *FASEB J.* **24**, 3903-3915.

Caldieri, G. and Buccione, R. (2010). Aiming for invadopodia: organizing polarized delivery at sites of invasion. *Trends Cell Biol.* **20**, 64-70.

Chabadel, A., Bañon-Rodríguez, I., Cluet, D., Rudkin, B. B., Wehrle-Haller, B., Genot, E., Jurdic, P., Anton, I. M. and Saltel, F. (2007). CD44 and beta3 integrin organize two functionally distinct actin-based domains in osteoclasts. *Mol. Biol. Cell* **18**, 4899-4910.

Chang, L., Jones, Y., Ellisman, M. H., Goldstein, L. S. and Karin, M. (2003). JNK1 is required for maintenance of neuronal microtubules and controls phosphorylation of microtubule-associated proteins. *Dev. Cell* **4**, 521-533.

Chen, S. Y. and Chen, H. C. (2006). Direct interaction of focal adhesion kinase (FAK) with Met is required for FAK to promote hepatocyte growth factor-induced cell invasion. *Mol. Cell. Biol.* **26**, 5155-5167.

Cheung, L. W., Leung, P. C. and Wong, A. S. (2006). Gonadotropin-releasing hormone promotes ovarian cancer cell invasiveness through c-Jun NH2-terminal kinase-mediated activation of matrix metalloproteinase (MMP)-2 and MMP-9. *Cancer Res.* **66**, 10902-10910.

Davis, R. J. (2000). Signal transduction by the JNK group of MAP kinases. *Cell* **103**, 239-252.

Denker, S. P., Huang, D. C., Orlowski, J., Furthmayr, H. and Barber, D. L. (2000). Direct binding of the Na – H exchanger NHE1 to ERM proteins regulates the cortical cytoskeleton and cell shape independently of H(+) translocation. *Mol. Cell* **6**, 1425-1436.

Destaing, O., Sanjay, A., Itzstein, C., Horne, W. C., Toomre, D., De Camilli, P. and Baron, R. (2008). The tyrosine kinase activity of c-Src regulates actin dynamics and organization of podosomes in osteoclasts. *Mol. Biol. Cell* **19**, 394-404.

Eferl, R. and Wagner, E. F. (2003). AP-1: a double-edged sword in tumorigenesis. *Nat. Rev. Cancer* **3**, 859-868.

Gupta, S., Barrett, T., Whitmarsh, A. J., Cavanagh, J., Sluss, H. K., Dérijard, B. and Davis, R. J. (1996). Selective interaction of JNK protein kinase isoforms with transcription factors. *EMBO J.* **15**, 2760-2770.

Heiska, L., Alfthan, K., Grönholm, M., Vilja, P., Vaheri, A. and Carpén, O. (1998). Association of ezrin with intercellular adhesion molecule-1 and -2 (ICAM-1 and ICAM-2). Regulation by phosphatidylinositol 4, 5-bisphosphate. *J. Biol. Chem.* **273**, 21893-21900.

Huang, C., Rajfur, Z., Borchers, C., Schaller, M. D. and Jacobson, K. (2003). JNK phosphorylates paxillin and regulates cell migration. *Nature* **424**, 219-223.

Kocher, H. M., Sandle, J., Mirza, T. A., Li, N. F. and Hart, I. R. (2009). Ezrin interacts with cortactin to form podosomal rosettes in pancreatic cancer cells. *Gut* **58**, 271-284.

Lee, H. H., Tien, S. C., Jou, T. S., Chang, Y. C., Jhong, J. G. and Chang, Z. F. (2010). Src-dependent phosphorylation of ROCK participates in regulation of focal adhesion dynamics. *J. Cell Sci.* **123**, 3368-3377.

Legg, J. W. and Isacke, C. M. (1998). Identification and functional analysis of the ezrin-binding site in the hyaluronan receptor, CD44. *Curr. Biol.* **8**, 705-708.

Linder, S., Wiesner, C. and Himmel, M. (2011). Degrading devices: invadosomes in proteolytic cell invasion. *Annu. Rev. Cell Dev. Biol.* **27**, 185-211.

Magalhaes, M. A., Larson, D. R., Mader, C. C., Bravo-Cordero, J. J., Gil-Henn, H., Oser, M., Chen, X., Koleske, A. J. and Condeelis, J. (2011). Cortactin phosphorylation regulates cell invasion through a pH-dependent pathway. *J. Cell Biol.* **195**, 903-920.

Manning, A. M. and Davis, R. J. (2003). Targeting JNK for therapeutic benefit: from junk to gold? *Nat. Rev. Drug Discov.* **2**, 554-565.

Matsui, T., Maeda, M., Doi, Y., Yonemura, S., Amano, M., Kaibuchi, K., Tsukita, S. and Tsukita, S. (1998). Rho-kinase phosphorylates COOH-terminal threonines of ezrin/radixin/moesin (ERM) proteins and regulates their head-to-tail association. *J. Cell Biol.* **140**, 647-657.

Murphy, D. A. and Courtneidge, S. A. (2011). The 'ins' and 'outs' of podosomes and invadopodia: characteristics, formation and function. *Nat. Rev. Mol. Cell Biol.* **12**, 413-426.

Ng, T., Parsons, M., Hughes, W. E., Monypenny, J., Zicha, D., Gautreau, A., Arpin, M., Gschmeissner, S., Verveer, P. J., Bastiaens, P. I. et al. (2001). Ezrin is a downstream effector of trafficking PKC-integrin complexes involved in the control of cell motility. *EMBO J.* **20**, 2723-2741.

Oshiro, N., Fukata, Y. and Kaibuchi, K. (1998). Phosphorylation of moesin by rho-associated kinase (Rho-kinase) plays a crucial role in the formation of microvilli-like structures. *J. Biol. Chem.* **273**, 34663-34666.

Pan, Y. R., Chen, C. L. and Chen, H. C. (2011). FAK is required for the assembly of podosome rosettes. *J. Cell Biol.* **195**, 113-129.

Pan, Y. R., Cho, K. H., Lee, H. H., Chang, Z. F. and Chen, H. C. (2013). Protein tyrosine phosphatase SHP2 suppresses podosome rosette formation in Src-transformed fibroblasts. *J. Cell Sci.* **126**, 657-666.

Ponta, H., Sherman, L. and Herrlich, P. A. (2003). CD44: from adhesion molecules to signalling regulators. *Nat. Rev. Mol. Cell Biol.* **4**, 33-45.

Roof, R. W., Dukes, B. D., Chang, J. H. and Parsons, S. J. (2000). Phosphorylation of the p190 RhoGAP N-terminal domain by c-Src results in a loss of GTP binding activity. *FEBS Lett.* **472**, 117-121.

Serrador, J. M., Alonso-Lebrero, J. L., del Pozo, M. A., Furthmayr, H., Schwartz-Albiez, R., Calvo, J., Lozano, F. and Sánchez-Madrid, F. (1997). Moesin interacts with the cytoplasmic region of intercellular adhesion molecule-3 and is redistributed to the uropod of T lymphocytes during cell polarization. *J. Cell Biol.* **138**, 1409-1423.

Serrador, J. M., Nieto, M., Alonso-Lebrero, J. L., del Pozo, M. A., Calvo, J., Furthmayr, H., Schwartz-Albiez, R., Lozano, F., González-Amaro, R., Sánchez-Mateos, P. et al. (1998). CD43 interacts with moesin and ezrin and regulates its redistribution to the uropods of T lymphocytes at the cell-cell contacts. *Blood* **91**, 4632-4644.

Simons, P. C., Pietromonaco, S. F., Reczek, D., Bretscher, A. and Elias, L. (1998). C-terminal threonine phosphorylation activates ERM proteins to link the cell's cortical lipid bilayer to the cytoskeleton. *Biochem. Biophys. Res. Commun.* **253**, 561-565.

Takino, T., Nakada, M., Miyamori, H., Watanabe, Y., Sato, T., Gantulga, D., Yoshioka, K., Yamada, K. M. and Sato, H. (2005). JSAP1/JIP3 cooperates with focal adhesion kinase to regulate c-Jun N-terminal kinase and cell migration. *J. Biol. Chem.* **280**, 37772-37781.

Tehrani, S., Faccio, R., Chandrasekar, I., Ross, F. P. and Cooper, J. A. (2006). Cortactin has an essential and specific role in osteoclast actin assembly. *Mol. Biol. Cell* **17**, 2882-2895.

Tsukita, S. and Yonemura, S. (1999). Cortical actin organization: lessons from ERM (ezrin/radixin/moesin) proteins. *J. Biol. Chem.* **274**, 34507-34510.

Tsukita, S., Oishi, K., Sato, N., Sagara, J., Kawai, A. and Tsukita, S. (1994). ERM family members as molecular linkers between the cell surface glycoprotein CD44 and actin-based cytoskeletons. *J. Cell Biol.* **126**, 391-401.

Tsuruta, F., Sunayama, J., Mori, Y., Hattori, S., Shimizu, S., Tsujimoto, Y., Yoshioka, K., Masuyama, N. and Gotoh, Y. (2004). JNK promotes Bax translocation to mitochondria through phosphorylation of 14-3-3 proteins. *EMBO J.* **23**, 1889-1899.

Whitmarsh, A. J., Cavanagh, J., Tournier, C., Yasuda, J. and Davis, R. J. (1998). A mammalian scaffold complex that selectively mediates MAP kinase activation. *Science* **281**, 1671-1674.

Wu, C. Y., Hsieh, H. L., Sun, C. C. and Yang, C. M. (2009). IL-1beta induces MMP-9 expression via a Ca2+-dependent CaMKII/JNK/c-JUN cascade in rat brain astrocytes. *Glia* **57**, 1775-1789.

Yao, K., Cho, Y. Y., Bergen, H. R., III, Madden, B. J., Choi, B. Y., Ma, W. Y., Bode, A. M. and Dong, Z. (2007). Nuclear factor of activated T3 is a negative regulator of Ras-JNK1/2-AP-1 induced cell transformation. *Cancer Res.* **67**, 8725-8735.

Yonemura, S., Hirao, M., Doi, Y., Takahashi, N., Kondo, T., Tsukita, S. and Tsukita, S. (1998). Ezrin/radixin/moesin (ERM) proteins bind to a positively charged amino acid cluster in the juxta-membrane cytoplasmic domain of CD44, CD43, and ICAM-2. *J. Cell Biol.* **140**, 885-895.

Yu, Q. and Stamenkovic, I. (1999). Localization of matrix metalloproteinase 9 to the cell surface provides a mechanism for CD44-mediated tumor invasion. *Genes Dev.* **13**, 35-48.

Yu, Q. and Stamenkovic, I. (2000). Cell surface-localized matrix metalloproteinase-9 proteolytically activates TGF-beta and promotes tumor invasion and angiogenesis. *Genes Dev.* **14**, 163-176.

Yu, W. H., Woessner, J. F., Jr, McNeish, J. D. and Stamenkovic, I. (2002). CD44 anchors the assembly of matrilysin/MMP-7 with heparin-binding epidermal growth factor precursor and ErbB4 and regulates female reproductive organ remodeling. *Genes Dev.* **16**, 307-323.

Supplemental Information

Phosphorylation of Moesin by c-Jun N-terminal Kinase Is Important for Podosome Rosette Formation in Src-transformed fibroblasts

Yi-Ru Pan, Wei-Shan Tseng, Po-Wei Chang, and Hong-Chen Chen

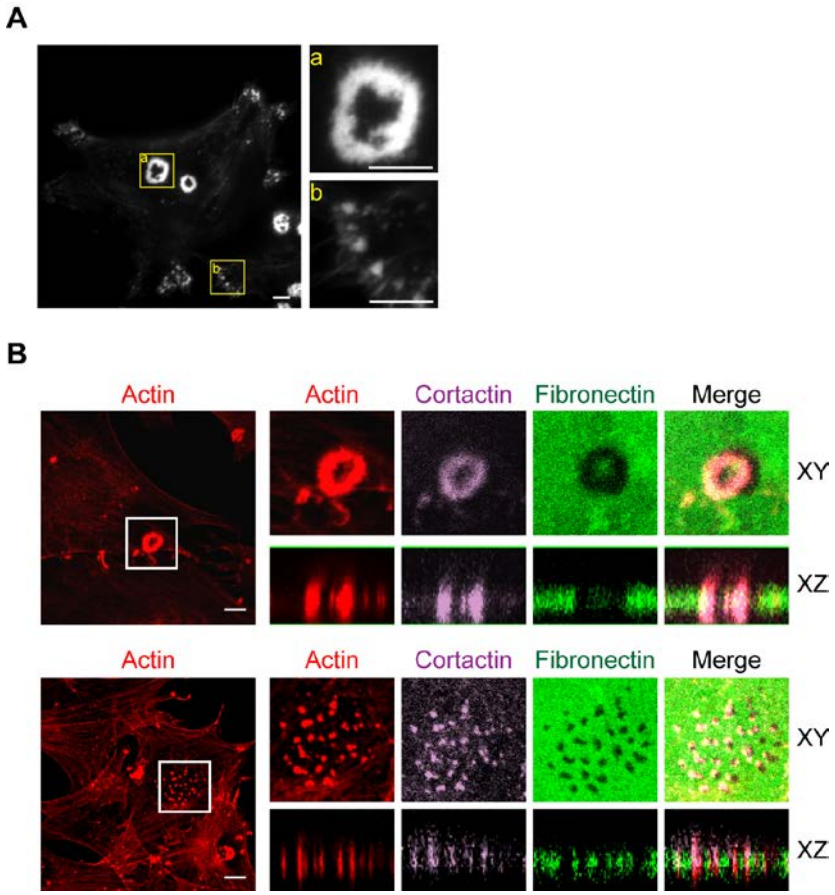

Figure S1. Rosette- and dot-like podosomes are detected at the ventral surface of SrcY527F-transformed NIH3T3 fibroblasts. (A) SrcY527F-transformed NIH3T3 cells were grown on fibronectin-coated glass coverslips for 24 h and then stained for F-actin. The images were captured by total internal reflection fluorescence microscopy. The boxed areas from the image are enlarged. The enlarged images from a podosome rosette (a) and podosome dots (b) are shown. Scale bar: 5 μm. **(B)** SrcY527F-transformed NIH3T3 cells were grown on Alexa Flour 488-conjugated fibronectin. The cells were fixed and stained for F-actin, cortactin, and nuclei. Z stack images were obtained and reconstructed by laser-scanning confocal microscopy. XY and XZ sections of the box containing a podosome rosette or podosome dots are enlarged. Scale bar: 10 μm.

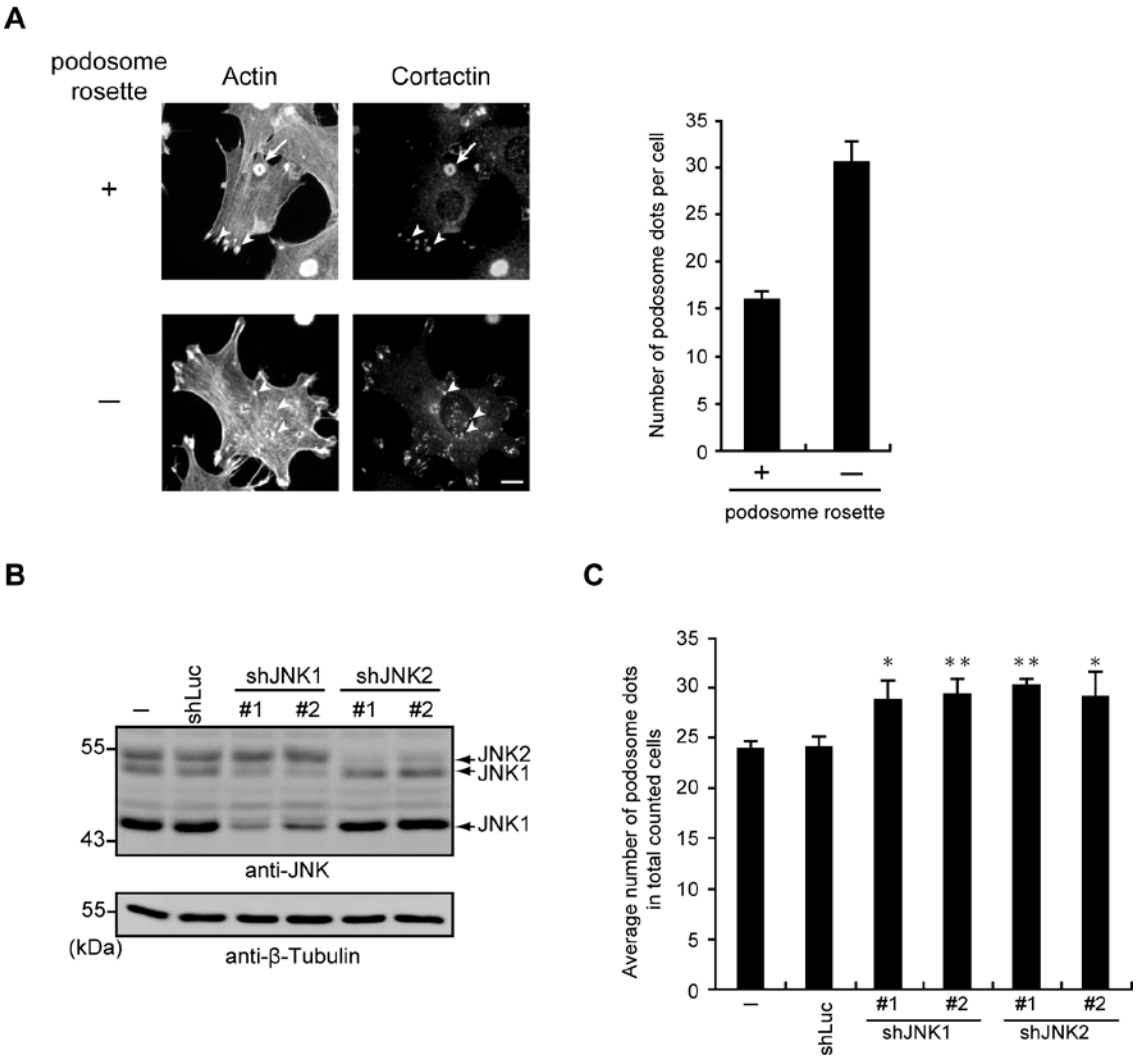

Figure S2. Depletion of JNK1 or JNK2 increases the number of podosome dots in SrcY527F-transformed NIH3T3 fibroblasts. **(A)** SrcY527F-transformed NIH3T3 cells were grown on fibronectin-coated glass coverslips for 24 h and were then stained for F-actin and cortactin. The images were selectively from the cell with (+) or without (-) podosome rosettes. Arrows indicate podosome rosettes. Arrowheads indicate podosome dots. Scale bar: 10 μm. Actin dots that co-localized with cortactin were considered to be podosome dots. The number of podosome dots in the cells with (+) or without (-) podosome rosettes was respectively counted (n=50). Values (means ± S.D.) are based on three independent experiments. **(B)** SrcY527F-transformed NIH3T3 cells were infected with lentiviruses encoding shRNAs specific to JNK1 (shJNK1; clones #1 and #2), JNK2 (shJNK2; clones #1 and #2) or luciferase (shLuc) as a control. An equal amount of whole cell lysates was analyzed by immunoblotting with the indicated antibodies. **(C)** The cells as in panel C were grown on fibronectin-coated glass coverslips for 24 h and then stained for F-actin and cortactin. Actin dots that co-localized with cortactin were considered to be podosome dots. The average number of podosome dots in the cells including those with and without podosome rosettes was measured (n=100). Values (means ± S.D.) are based on three independent experiments. **, $P < 0.005$; *, $P < 0.05$.

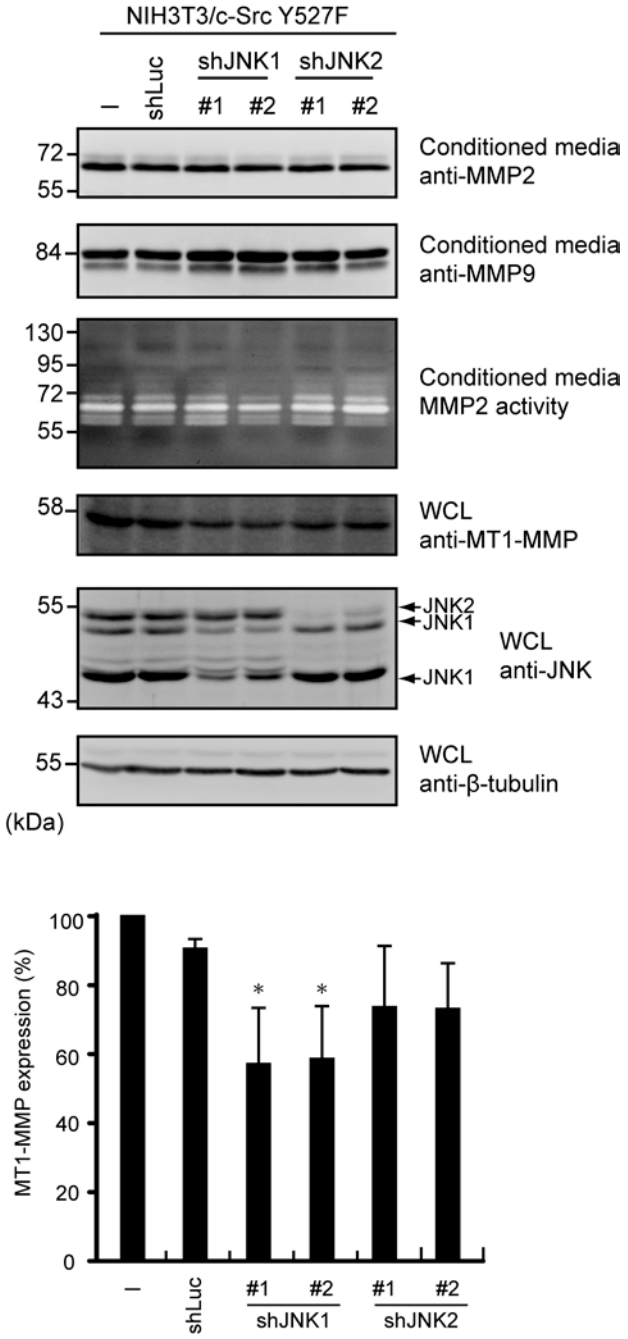

Figure S3. Depletion of JNK decreases the expression of MT1-MMP in Src-transformed NIH3T3 fibroblasts. An equal amount of whole cell lysates (WCL) or conditioned media from SrcY527F-transformed NIH3T3 cells expressing shRNAs specific to JNK1 (shJNK1; clones #1 and #2), JNK2 (shJNK2; clones #1 and #2), or luciferase (shLuc) was analyzed by immunoblotting with the indicated antibodies. The activity of MMPs in the conditioned media was analyzed by a gelatin zymography. The expression of MT1-MMP was quantified and expressed as the percentage relative to the level in control SrcY527F-transformed NIH3T3 cells, which was defined as 100%. Values (means ± S.D.) are based on three independent experiments. *, $P < 0.05$.

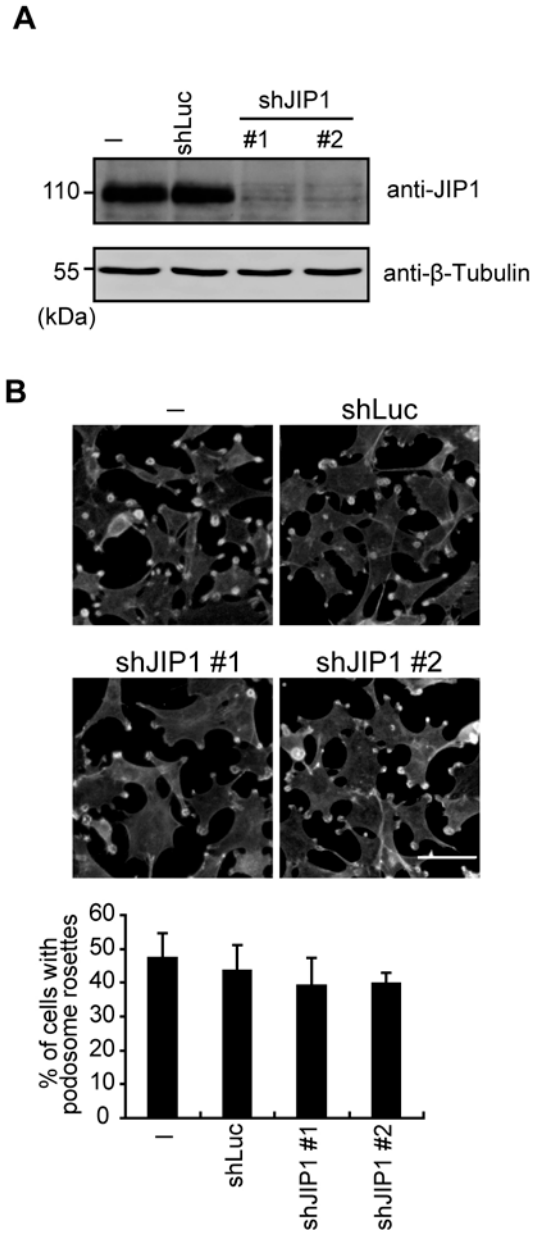

Figure S4. JIP1 is not involved in the formation of podosome rosettes in SrcY527F-transformed NIH3T3 fibroblasts. (A) An equal amount of whole cell lysates from SrcY527F-transformed NIH3T3 cells expressing shRNAs specific to JIP1 (shJIP1; clones #1 and #2) or luciferase (shLuc) was analyzed by immunoblotting with the indicated antibodies. (**B**) The cells as in panel A were grown on fibronectin-coated glass coverslips for 24 h and then stained for F-actin. The percentage of cells containing podosome rosettes in the total number of counted cells ($n \geqq 200$) was determined. Values (means ± S.D.) are based on three independent experiments.